Effects of Hypocalcemic Vitamin D Analogs in the Expression of DNA Damage Induced in Minilungs from Hescs: Implications for Lung Fibrosis

Esmeralda Magro-Lopez
Carlos III Health Institute: Instituto de Salud Carlos III
Irene Chamorro-Herrero
Carlos III Health Institute: Instituto de Salud Carlos III
Alberto Zambrano (azambra@isciii.es)
Instituto de Salud Carlos III Campus de Majadahonda https://orcid.org/0000-0001-5677-2999

Research

Keywords: human pluripotent stem cells, hESCs, minilungs, vitamin D; vitamin D analogs, paricalcitol, calcipotriol, lung fibrosis.

Posted Date: November 11th, 2021

DOI: https://doi.org/10.21203/rs.3.rs-1030901/v1

Abstract

Background

In our previous work, we evaluated the therapeutic effects of 1α,25-Dihydroxyvitamin D_3, the biologically active form of vitamin D, in the context of bleomycin-induced lung fibrosis. Contrary to the expected, vitamin D supplementation increased DNA damage expression and cellular senescence in alveolar epithelial type II cells and aggravated the overall lung pathology induced in mice by bleomycin. These effects were probably due to an alteration of the cellular DNA double-strand breaks repair capability. In the present work we have evaluated the effects of two hypocalcemic vitamin D analogs (calcipotriol and paricalcitol) in the expression of DNA damage in the context of minilungs derived from human embryonic stem cells and in the cell line A549.

Results

As in the case of the cell line A549, bleomycin can induce DNA damage in the generated minilungs enriched in alveolar cells. The results indicate that, in contrast to vitamin D, the treatment of the minilungs with the hypocalcemic analogs reduce significantly the bulk of DNA damage expression in both bidimensional arrays of epithelial cells (2D minilungs) and lung bud organoids (3D minilungs). The initial evaluation of a battery of commercially available vitamin D analogs shows a significant reduction in A549 cells of gH2AFX expression levels, a marker of DNA damage, cell senescence and aging.

Conclusions

The treatments based in hypocalcemic vitamin D analogs might be used to reduce the bulk of DNA damage and eventually the subsequent cell senescence expression that underlie lung conditions as those that can evolve with fibrosis.

Background

DNA damage and cellular senescence underlie the physiopathology associated to idiopathic pulmonary fibrosis (IPF) and other chronic conditions that can evolve with fibrosis. IPF is a form of progressive interstitial pneumonia of unknown etiology with an estimated survival of 3-4 years (1). IPF pathogenesis is the consequence of an excessive matrix deposition leading to tissue scarring and irreversible organ injury probably due to a persistent input of damage and tissue repair response. It has been reported that cellular senescence is implicated in the tissue repair program and its occurrence in IPF, unfortunately, has a detrimental role in contrast to other fibrogenic conditions (2) (3) (4). Vitamin D and its analogs have been proved to be active in the regulation of fibrosis that characterizes multiple chronic diseases including pulmonary fibrosis (5) (6) (7) (8). For instance, the preventive use preventive of vitamin D supplementation was associated to a general improvement of the lung fibrosis symptomatology induced in mice probably due to its anti-inflammatory effects (8) (9). However, as we have reported in our previous work, the “therapeutic” treatment of mice having bleomycin-induced fibrosis seemed to worsen the

pathology: the mice treated with vitamin D showed increased architectural distortion, subpleural scarring and more areas of aberrant reepithelization compared to controls. These areas were defined by the accumulation of alveolar epithelial type II (ATII) cells harboring high levels of DNA damage in the form of double strand breaks (DSBs). DSBs were also observed in cells throughout respiratory bronchioles or immersed in alveolar fields. The bulk of DNA damage was preferably associated to epithelial cells; fibroblasts, however seemed to be more resistant to DNA damage than epithelial cells (10). Senescence can be induced prematurely as a result of a persistent DNA damage response (DDR) secondary to oxidative stress that induces double-strand breaks DSBs (11). Indeed, DSBs are potent inducers of cell arrest and a typical hallmark of cell senescence (12). Our results also showed significant greater levels of DSBs and cell senescence in epithelial cells than in fibroblasts and were consistent with the central hypothesis underlying IPF indicating that epithelial injury and impaired regeneration activate fibroblasts and that cellular senescence induced by persistent epithelial damage may be the origin of aberrant epithelial regeneration and the promotion of fibrosis (13) (14) (15) (16).

In the present study we have evaluated various vitamin D analogs in the context of DNA damage induced by sublethal doses of bleomycin. A huge amount of vitamin D analogs have been synthesized during the years and their clinical use for secondary hyperparathyroidism, osteoporosis or psoriasis has been approved for many of them (17) (18). The potent effect of vitamin D on intestinal calcium and phosphorus absorption and bone mineral mobilization often leading to the development of hypercalcemia and hyperphosphatemia has precluded its therapeutic use for many conditions. The ideal analog would retain vitamin D receptor binding capacities and have minimal effects on calcium and phosphorus metabolism. Our working hypothesis is that hypocalcemic vitamin D analogs could show a lower incidence in the expression of DNA damage upon a bleomycin insult than the active form of vitamin D.

Results

We have tested our postulated hypothesis in the cell line A549, an immortalized counterpart of ATII cells, in 2D minilungs (lung and alveolar differentiated cells from hESCs arranged in bidimensional cultures) and in 3D minilungs from hESCs (human lung bud organoids embedded in Matrigel^{TM} sandwiches). Lung organoids generated from hESCs have enormous advantages over cell lines or simple primary cultures as they offer an unlimited availability of primary cells, they show the complete lung epithelial spectrum and emulate structural and functional features of the original organ.

The exposure of A549 cells to a sublethal bleomycin shock (12µg/mL for 6 h) induces the expression of DNA damage (DD) foci containing TP53BP1, a reliable marker of DSBs (19) (20) (21) (22) (23). These conditions allow the accurate quantification of DSBs. DD foci are rapidly visualized as discrete foci in a pan-nuclear pattern (Figure 1A). As previously reported (10) , the exposure of A549 cells to vitamin D, in the presence of bleomycin, increased the levels of DD foci, both the percentage of damaged cells and the levels of severely damaged cells harboring more than 20 DD foci per nucleus (Figure 1B-D) (n=3; >150 cells were analyzed; P<0,001). However, the two hypocalcemic vitamin D analogs tested (paricalcitol and

calcipotriol) were able to drastically reduce the bulk of DD expression compared to vitamin D in the presence of bleomycin (Figure 2C-D; n=3; >150 cells were analyzed; ANOVA P<0,001). Figure 2A-B shows that the treatment of A549 cells with vitamin D or its analogs, in the absence of bleomycin, did not alter the low basal level of damage of the cell population as previous described for vitamin D (10) (n=3; >150 cells were analyzed; ANOVA P<0,001). In order to reproduce these results in much more reliable models of lung structure and function we generated minilungs from hESCs as previously described (24) (25). By one hand we generated lung airway and epithelial cells arranged in bidimensional cultures (2D minilungs) from the hESC line AND-2 as previously described (24). Briefly, good hESCs colonies are grown along inactivated MEFs (iMEFs), picked-up and passaged to new plates with MEFsi in order to accumulate material for lung differentiation. Figure 3A shows the expression of pluripotency marker SOX-2 in a good AND-2 colony and representative micrograph at various times of the differentiation process: embryoid bodies (EBs), anterior foregut endoderm (AFE), cultures at day 23 (lung progenitors) and at day 60 (differentiated lung airway and alveolar cells). Cultures from day 50 onwards show the expression of representative markers of lung airway and alveolar cells illustrating the heterogeneity in cell shape including the presence of flat cells with a crescent shape morphology, and granular and roughly cuboidal-shaped cells, likely corresponding to ATI and ATII cells, respectively (Figure 3A; d60). Although from day 50 they can be considered mature we the cultures were used for the desired experimentation from day 60 on. Figure 3B shows a RT-qPCR result illustrating the complexity of these cultures (n=3; > 4 organoids per experimental replicate were used). As previously described by us and others (24) (25) (26) (27) (28), the differentiation protocol applied yields cultures enriched in alveolar epithelial cells (ATI and ATII cells). By other hand, the generation of 3D minilungs implies the formation of nascent organoids in suspension at certain time of the protocol (see material & methods for details) (Figure 3C) and their final embedding in Matrigel™ sandwiches to reach the desirable state of differentiation characterized by the presence of lung buds more or less branched [lung buds organoids (LBOs)] as previously described (25) (28) (Figure 3D). Figure 3E shows representative micrographs of histochemical analysis (H&E staining) and immunohistochemical analysis with surfactant antibodies performed on LBOs sections. In order to analyze the expression of DNA damage and the effect of vitamin D and its analogs, 2D minilungs were treated with 12.5 µg/mL of bleomycin for 72h due to the heterogeneity and density of these cultures. All the cell types of these complex cultures seemed to be affected equally by the bleomycin treatment. As in the case of A549 cells, neither vitamin D nor its hypocalcemic analogs altered significantly the basal levels of DD in the absence of bleomycin (Figure 4A-B) (n=3; >150 cells were analyzed; ANOVA P<0,001). As expected, the exposure of these cultures to bleomycin and vitamin D increased the levels of DD foci reached by bleomycin itself (Figure 4C-D). As in the case of A549 cells, the treatment with paricalcitol and calcipotriol not only did not they further increase the DD levels reached by bleomycin, but they seemed to reduce significantly the DD expression induced by bleomycin (Figure 4C-D, (n=3; >4 organoids per condition were used and >150 cells were analyzed; ANOVA P<0,001). Equivalent assays were performed on 3D minilungs except the concentration of bleomycin used (25 µg/mL instead of 12,5 µg/mL) with the idea that enough bleomycin could reach the embedded material. As previously reported, lung buds minilungs are mainly constituted by ATII cells (28) (25). Although to a lesser extent we found similar results to those obtained in the case of 2D minilungs (Figure 4E-H) (n=3; >4 organoids per condition were

used and >150 cells were analyzed; ANOVA P>0,05 (panels 4E-F) and ANOVA P<0,001 for data represented in panels 4G-H). Finally, we evaluate in A549 cells, a continuous cell line counterpart of ATII cells, the expression of gH2AFX marker which is a reliable marker of DD, cell senescence and aging, as previously described (22) (29) (22). Figure 4I shows the significant increase in gH2AFX expression levels in the presence of bleomycin and vitamin D compared to controls and the drastic reduction induced by paricalcitol. Equivalent assays were performed using a battery of commercially available less hypercalcemic vitamin D analogs including 22-oxacalcitriol, tacalcitol and vitamin D2. All the vitamin D analogs seemed not to further increase the expression levels of gH2AFX reached in bleomycin treated cells (Figure 4J). Moreover, in the case of paricalcitol, a significant reduction in the expression of gH2AFX compared to bleomycin treated cells is observed.

Discussion

The generation of human minilungs which share the structural features and some extent of the functionality of the native organ may serve as system model to emulate the DNA damage inflicted during the course of fibrogenic conditions such as IPF. Currently, the more efficient protocols to generate airway and alveolar epithelial cells from the direct differentiation of hPSCs are biased to the production of alveolar cells (28) (26) (25). Bleomycin seems to inflict DNA damage in the form of DSBs in all the epithelial cells equally, even when the cell organization is the form of lung buds embedded in Matrigel^{TM} sandwiches. Altogether the initial results presented here suggest that less hypercalcemic analogs don't show the deleterious effects observed by vitamin D treatment in the presence of bleomycin and could be an alternative to vitamin D supplementation. In addition, the treatment with this kind of vitamin D analogs could be tested as efficient agents to reduce the bulk of DD expression underlying multiple diseases that can evolve with DNA damage, fibrosis and aging such as IPF and other lung interstitial conditions.

Material And Methods

Cell culture

Alveolar epithelial cells type II (A549, ATCC) were maintained in DMEM medium supplemented with 10% FBS (Sigma), 2mM glutamine and 100U/mL of penicillin and streptomycin (Lonza). We used the active form of vitamin D (1α,25-Dihydroxyvitamin D_3 or calcitriol) (cat.#D1530; Sigma-Aldrich; Vitamin D stock was 10 µM in ethanol) and the following vitamin D analogs (stocks were 50 µM in ethanol): calcipotriol (cat.#203537; Santa Cruz Biotechnology), paricalcitol (cat.#477938; Santa Cruz Biotechnology), tacalcitol (cat.#sc-361371a; Santa Cruz Biotechnology), 22-Oxacalcitriol (cat.#sc-361076; Santa Cruz Biotechnology) and vitamin D2 (cat.#sc- sc-205988; Santa Cruz Biotechnology). Treatments were performed in cells maintained in DMEM supplemented with 10% hormone-depleted serum. This serum was prepared by using the anion exchange resin AGR1-X8 from BIO-RAD (cat.#1401441) as previously described (22). Bleomycin sulfate (cat.# CAYM13877–50) was purchased to VWR (Bleomycin stock: 50 mM in PBS).

Maintenance of hESCs

The hESCs line AND-2 was obtained from the "Biobanco de células madre de Granada" (ISCIII, Spain); passages 26-40. Mouse embryonic fibroblasts (MEFs) were obtained at 13.5 days post-coitum from C57BL/6 mice as described previously (22). MEFs were mitotically inactivated by an overnight treatment with 2 µg/mL of mitomycin C (cat.#M4287; Sigma-Aldrich) and plated at a density of approximately 16000 cells/cm^2. hESCs were cultured along with MEFs under standard conditions (http://www.stembook.org). The maintenance medium was composed of KO-DMEM (cat.#10829-018 Gibco; Life Technologies), 20% KO serum replacement (cat.#10828010 Gibco; Life Technologies), 0,1 mM β-mercaptoethanol (cat.#21985-023 Gibco; Life Technologies), 2 mM Glutamax (cat.#35050-061,Gibco; Life Technologies), nonessential aminoacids (cat.#11140-050 Gibco; Life Technologies and primocin (cat.#12I05MM; InvivoGen). The medium was filtered by using 0,22-µ pore filter systems (cat.#431097; Corning); 10 ng/mL recombinant human basic Fibroblast Growth Factor (hbFGF) (cat.#PHG6015; Invitrogen) and 10 µM Y-27632 (cat.#1254; Tocris R&D Systems) were added before use. The medium was changed in a daily basis and cells were passaged either by enzymatic (collagenase IV method) (collagenase IV: cat.#11140050; Gibco; Life Technologies) or mechanical procedures (http://stembook.org). Cells were maintained in an undifferentiated state in a 5% CO_2/air environment. The differentiation process was carried-out in a 5% CO_2/5% O_2/95% N_2 environment [Galaxy 48R incubator (New Brunswick)], unless otherwise indicated.

Primitive streak formation and induction of definitive endoderm (DE)

Induction of endoderm was performed as previously described (Magro-Lopez et al., 2018, 2017). Primitive streak formation (day 0; 24h) and endoderm induction (days 1-4) were performed in serum-free differentiation (SFD) medium. SFD medium was composed of a mix of IMDM:F12 (3:1) media (cats.#B12-722F and 10-080 CVR; Corning), supplemented with N2 (cat.#17502-048, Gibco; Life Technologies), B27 (cat.#17504-044, Gibco; Life Technologies), 2 mM Glutamax (cat.#35050-061 Gibco; Life Technologies), 1% penicillin-streptomycin (DE17-602E; Lonza), and 0.05% bovine serum albumin (BSA) (cat.#A7906; Sigma-Aldrich). The medium was filtered using a 0.22 µ-pore filter system (cat.#431097; Corning); 50 µg/mL ascorbic acid (cat.#A4554; SigmaAldrich) and 0.04 µL/mL monothioglycerol (stock >97%) (cat.#M6145; Sigma-Aldrich) were added before use. MEFs were depleted by passaging hESCs lines onto Matrigel™-coated (cat.#354230; Life Technologies) plates for at least 48h. Cells were briefly trypsinized into small 3-10 cell clumps and the reaction was halted with stop medium [IMDM medium (BE12722F) supplemented with 50% foetal bovine serum (F7524, Sigma-Aldrich), 2 mM Glutamax, 1% penicillin-streptomycin and 30 ng/mL DNase I (cat.#260913-10MU; Calbiochem)]. Cells were then centrifuged 5 min at 850 rpm and washed carefully two times with an excess of SFD medium. To form embryoid bodies (EBs), the clumps were plated onto low-attachment 6-well plates (cat.#3471; Corning) and maintained in SFD medium in a 5% CO_2/5% O2/95% N_2 environment (Galaxy 48R incubator; New Brunswick).

For primitive streak formation, 10 μM Y-27632, 10 ng/mL Wnt3a (cat.#5036-WN; R&D Systems) and 3 ng/mL human BMP4 (cat.#314-BP; R&D Systems) were used. EBs were collected, resuspended carefully in endoderm induction medium containing 10 μM Y-27632, 0.5 ng/mL human BMP4, 2.5 ng/mL hbFGF, and 100 ng/mL human Activin (cat.# 338-AC; R&D Systems). Cells were fed after 36–48 h, depending on cell density, by removing half the old medium and adding half fresh medium.

Induction of anterior foregut endoderm (AFE)

AFE (days 4, 5 or 5) was induced as previously described (Magro-Lopez et al., 2018, 2017). EBs were dissociated into single cells with trypsin. Dissociated cells were transferred to a conical tube containing stop medium to neutralize trypsin. Cells were centrifuged for 5 min at 850 rpm, washed carefully twice with SFD medium and counted. For AFE induction, 25.000-30.000 cells/cm^2 were plated on fibronectin–coated (F0895; Sigma-Aldrich) 12-well tissue culture plates in AFE induction medium 1 [SFD medium supplemented with 10 mM SB-431542 (cat.#1614; Tocris) and 100 ng/mL of NOGGIN (cat.#6057;, R&D Systems). After 24h of incubation, the medium was aspirated and AFE induction medium 2 [SFD medium supplemented with 1 μM IWP2 (cat.#3533; Tocris) and 10 μM of SB-431542] was added to the cultures. This process was carried out under hypoxic conditions only for bidimensional cultures.

Lung progenitors induction and expansion

Lung progenitor induction and expansion was carried out as previously described (Magro-Lopez et al., 2018, 2017). On day 6,5-7, AFE cultures treated for 20 days with the ventralization medium consisting of SFD medium supplemented with 3 μM CHIR99021 (cat.#04; Tocris), 10 ng/mL human FGF10 (cat.#345-FG; R&D Systems), 10 ng/mL human KGF (cat.#251KG-010; R&D Systems), 10 ng/mL human BMP4 (cat.#314-BP; R&D Systems), 10 ng/mL murine EGF (cat.#2028-EG-200; R&D Systems) and 50 nM all-trans retinoic acid (cat.#R2625; Sigma-Aldrich). Culture medium was changed every two days. At a time point between days 8 to 12 cultures were incubated under normoxic conditions. At day 16, cultures were briefly digested with trypsin in order to remove potential nonectodermal contaminating cells. Supernatant of this brief digestion containing single cells and small clumps were removed. The remaining cell clumps were replated onto fibronectin-coated MW12 plates at 1:3 dilutions in fresh medium after trypsin neutralization and careful washing. Plates were returned to the hypoxic conditions (5% CO_2/5%O_2/95%N_2 environment).

Lung and airway epithelial cells maturation

At day 26 cultures were incubated with SFD medium supplemented with 3 μM CHIR99021, 10 ng/mL human FGF10, 10 ng/mL human FGF10, 0,1 mM 8-bromocAMP (cat.# B5386; Sigma-Aldrich), 0,1 mM IBMX (3,7-dihydro-1-methyl-3-(2methylpropyl)-1H-purine-2,6-dione; cat.# I5879; Sigma-Aldrich)) and 60 nM dexamethasone (cat.#D5902; Sigma-Aldrich). The medium was changed every two days and plates were maintained under conditions (5%CO_2/5%O_2/95%N_2 environment). Cultures were carried further in these conditions until their experimental use at day 50. Treatments were performed in minilungs maintained in day 26 medium as indicated in the corresponding experiments.

Formation of lung bud organoids

In this case, the differentiation process was performed under normoxic conditions from the anteriorization stage on. At day 8, cells were briefly trypsinized into small 3–10 cell clumps and the reaction was halted with stop medium (IMDM medium (BE12-722F) supplemented with 50% fetal bovine serum (FBS; F7524; Sigma-Aldrich), 2 mM Glutamax, 1% penicillin-streptomycin). Cells were then centrifuged for 5min at 850 rpm and washed carefully twice with an excess of SFD medium. The clumps were plated onto low-attachment six-well plates (cat.#3471; Corning) in branching medium (SFD medium containing 3 μM CHIR99021, 10 ng/mL FGF10, 10 ng/mL KGF, 10 ng/mL BMP4, 50 nM all-trans retinoic acid). These three-dimensional clumps (nascent lung bud organoids) were incubated and fed every other day for approximately 20–25 days. After that, these nascent organoids were embedded into a Matrigel^{TM} sandwich assembled on MW96 wells. 50 μL of Matrigel^{TM} was loaded on the MW96 well and allowed to gel. Nascent organoids were picked up with a wide mouth plastic Pasteur pipette, divided into MW96 wells containing 50% Matrigel^{TM}, diluted in branching media and immediately transferred onto the first layer of Matrigel^{TM}. After solidification of this intermediate layer containing the nascent organoids, 50 μLMatrigel^{TM} was added on top. Finally, each sandwich containing various organoids was incubated with 50 μL branching media. Medium was changed every 2–3 days. Growing branching structures were easily visualized under the microscope after 1 or 2 weeks. Treatments were performed in minilungs maintained in branching medium as indicated in the corresponding experiments.

Indirect immunofluorescence of A549 cells and 2D minilungs

Cells were seeded in 8-well chambers (cat.#154,534; Thermofisher Scientific) at a density of 20.000 cells/well. The following day the cells were treated as indicated in the corresponding experiments. Immunofluorescence was performed as previously described (Zambrano et al., 2014). Basically, cells were fixed in 2% PFA in PBS for 10min at RT and permeabilized with 0.1% Triton X-100 and 0.1% sodium citrate for 5min at RT. Preparations were washed with PBS and washing solution (PBS/0.25% BSA/0.1% Tween 20), blocked for 30 min with blocking solution (washing solution + 2.5% BSA), and incubated overnight with antibodies against TP53BP1(1:500; sc-16565; Invitrogen). Preparations were then washed with washing solution and incubated with secondary antibodies conjugated with alexa fluor dyes (488, 546) from Life Technologies (cat.#A-11029, cat.#A-11035) for 1h at RT. Nuclei were counterstained with DAPI, and samples were mounted with ProLong Diamond (cat.#P36961; Life Technologies). Cell images were captured with a fluorescence microscopy (Zeiss Axio) equipped with a camera (AxiocamMRm) and AxioVision software. DNA damage foci were quantified by counting from >150 cells for each experimental condition. For 2D minilungs, the glass chamber slides were incubated overnight at 4ºC with human fibronectin in order to plate the differentiated cells. Cultures from day 50 were digested with trypsin, neutralized with stop medium and washed with SFD medium. Approximately 40.000 differentiated epithelial cells per well were plated in the epithelial maturation medium. Cultures were maintained in normoxic conditions for one day before treatments.

Indirect immunofluorescence of lung bud organoids

Organoids were picked up from the MW96 wells, transferred into a well of a MW12 and fixed with 4% paraformaldehyde (PFA) for 15 min at RT. After that, the organoids were washed three times with PBS for 10 min and incubated overnight at 4°C with 30% sucrose. The sucrose was exchanged for a solution of 7.5% gelatin/15% sucrose and incubated for 15 min at 37°C. The organoids were carefully transferred to cryomolds and progressively embedded in various layers of solidified 7.5% gelatin/15% sucrose. These preparations were cut into 10-µm sections in a Leica CM3050 cryostat. The mounted sections were washed with PBS and permeabilized with PBS/1% BSA/0.25% Triton X-100 for 5 min at RT. After that, the sections were washed and blocked for 30min at RT with blocking solution (PBS-BSA 1%). The sections were incubated for 2h with antibodies against TP53BP1 (1:500; sc-16565; Invitrogen) or the pro surfactant protein C (1:200; ab3785, Merck). Preparations were washed with washing solution and incubated with a secondary antibody conjugated with Alexa fluor dye (546) from Life Technologies (cat.#A-11035) for 1h at room temperature. Nuclei were counterstained with DAPI and samples were mounted with ProLong Diamond (cat.#P36961; Life Technologies). Cell images were captured with a fluorescence microscopy (Zeiss Axio) equipped with a camera (AxiocamMRm) and AxioVision software. DNA damage foci were counted from >150 cells for each experimental condition.

Analysis of proteins by western-blot

Cell monolayers were washed with ice-cold PBS and lysed in triple-detergent lysis buffer [50 mM Tris-HCl pH 8.0, 150 mM NaCl, 0.02% sodium azide, 0.1% SDS, 1% NP-40, 0.5% sodium deoxycholate, 100 µg/ml PMSF, 2 µg/ml pepstatin, 2 µg/ml aprotinin, 2 µg/ml leupeptin, and phosphatase inhibitors cocktail 2 or 3 (cat.#P5726, P0044, Sigma-Aldrich)]. SDS-PAGE and immunoblotting were performed under standard conditions. Basically, samples in Laemmli buffer (30 µg/lane) were separated through 12% gels and transferred to nitrocellulose membranes for 90 min at RT in the presence of 20% methanol and 0,1% SDS. Membranes were blocked with 3% BSA in PBS-Tween 0,05% (PBST-BSA) and incubated O/N at 4 °C with a γH2AFX antibody (cat.#05–636, Millipore) diluted 1:1000 in PBST-BSA. Densitometry analysis of bands was performed by using Image J software (https://imageJ.nih.gov/)

Quantitative real-time RT-PCR (RT-qPCR) of minilungs

Total RNA was extracted using Trizol (cat.#15596026; Ambion) following manufacturer's instructions. cDNA was generated using the High-Capacity cDNA kit (cat.#4387406; Applied Biosystems). Real-time qPCR was performed by using the powerUpSYBR Green mix (cat.#A25742) on the Quantstudio-3 system (Applied Biosystems) following manufacturer's instructions. Absolute quantification of each gene was obtained using a standard curve of serial diluted genomic DNA (cat.#11807720, Roche) and normalized to housekeeping gene TBP (Tata Box Binding protein)

The genes analyzed and the sequences of the oligonucleotides employed in this study, were the following: *TBP* [Tata-Box Binding Protein; Forward: 5'-TGAGTTGCTCATACCGTGCTGCTA, Reverse: 5'-CCCTCAAACCAACTTGTCAACAGC]; *TP63* (Tumor Protein P63, marker of basal cells) [Forward: 5'-CCTATAACACAGACCACGCGCAGA, Reverse: 5'-GTGATGGAGAGAGAGCATCGAAG]; *MUCIN5AC* (Mucin 5AC, marker of globet cells) [Forward: 5'GCACCAACGACAGGAAGGATGAG, Reverse: 5'-

CACGTTCCAGAGCCGGACAT]; *SCGB1A1* (Secretoglobin Family1A Member1 or CC10, marker of clara cells) [Forward: 5'-TCATGGACACACCCTCCAGTTATGAG,

Reverse: 5'-TGAGCTTAATGATGCTTTCTCTGGGC]; *PDPN* (Podoplanin, marker of AT-I cells) [Forward: 5'-AGGAGAGCAACAACTCAACGGGA, Reverse: 5'- TTCTGCCAGGACCCAGAGC]; *AQP5* (Aquaporin 5, marker of AT-I cells) [Forward: 5'- GCCATCCTTTACTTCTACCTGCTC, Reverse: 5'-GCTCATACGTGCCTTTGATGATGG]; *SFTPA* (Surfactant Protein A, marker of AT-II cells) [Forward: 5'-GTGCGAAGTGAAGGACGTTTGTG, Reverse: 5'-TTTGAGACCATCTCTCCCGTCCC]; *SFTPB* (Surfactant Protein B, marker of AT-II cells) [Forward: 5'-TCTGAGTGCCACCTCTGCATGT, Reverse: 5'-TGGAGCATTGCCTGTGGTATGG]; *SFTPC* (Surfactant Protein C, marker of AT-II cells) [Forward: 5'-CCTTCTTATCGTGGTGGTGGTGGT, Reverse: 5'-TCTCCGTGTGTTTCTGGCTCATGT]; *SFTPD* (Surfactant Protein D, marker of AT-II cells) [Forward: 5'-TGACTGATTCCAAGACAGAGGGCA, Reverse: 5'-TCCACAAGCCCTGTCATTCCACTT]; *FOXJ1* (Forkhead Box J1, marker of ciliated cells) [Forward: 5'-GGCATAAGCGCAAACAGCCG, Reverse: 5'-TCGAAGATGGCCTCCCAGTCAAA]

Statistical analysis

Data were subjected to the Shapiro-Wilk test and D'Agostino and Pearson omnibus test to verify their normality. Statistical significance of data was determined by applying a two-tailed Student's t test or analysis of variance followed by the Newman–Keuls or Bonferroni post-tests for experiments with more than two experimental groups. $P < 0.05$ is considered significant. Significance of analysis of variance post-test or the Student's t test is indicated in the figures as *, $P < 0.05$; **, $P < 0.01$; and ***, $P < 0.001$. Statistics were calculated with the Prism 7 software (GraphPad Software). The results presented in the figures are means ±SEM. Experiments were repeated three times.

Abbreviations

AFE	Anterior Foregut Endoderm
ATI	Alveolar Type I Cells
ATII	Alveolar Type II Cells
BMP4	Bone Morphogenic Protein 4
BSA	Bovine serum albumin
DD	DNA damage
DD foci	DNA damage foci
DSBs	DNA double-strand breaks
EBs	Embryoid Bodies
FBS	Foetal bovine serum
FGF	Fibroblast Growth Factor
FOXJ1	Forkhead Box J1
H2AFX	H2A histone family member X
hbFGF	Human basic fibroblast growth factor
hESCs	Human Embryonic Stem Cells
hPSCs	Human Pluripotent Stem Cells
IBMX	Isobutylmethylxanthine
IPF	Idiopathic Pulmonary Fibrosis
KGF	Keratinocyte growth factor
LBOs	Lung bud organoids
MEFs	Mouse Embryonic Fibroblasts
MUCIN5AC	Mucin 5AC, Oligomeric Mucus/Gel-Forming
PBS	Phosphate-buffered saline
PDPN	Podoplanin
RT-qPCR	Quantitative Real-Time RT-PCR (Reverse Transcription Polymerase Chain Reaction)
SCGB1A1	Secretoglobin Family 1A Member 1; CC10
SEM	Standard error of the mean
SFD	Serum-free differentiation
SFTPA	SurfactantProtein A

SFTPB	SurfactantProtein B
SFTPC	SurfactantProtein C
SFTPD	SurfactantProtein D
SOX2	SRY (Sex Determining Region Y)-box 2
TBP	TATA Box Binding Protein
TP53BP1	Tumor Protein P53 Binding Protein 1
TP63	Tumor Protein p63
µm	Micrometer

Declarations

Ethics approval and consent to participate

The use of the hESC line AND-2 and the experimental procedures of this study were approved by the ISCIII Ethics Committee (ref. no. CEI PI 10_2015-v2) and the National Committee of Guarantees for the Use and Donation of human Cells and Tissues (ref. no. 345 288 1 and 436 351 1).

Consent for publication

Not applicable

Availability of data and materials

Please contact the corresponding author for data requests.

Competing interests

The authors have not conflict of interests to declare

Funding

This work was supported by the Grant PI19CIII/00003 from the Institute of Health Carlos III (ISCIII) to Alberto Zambrano.

Authors' contributions

EM-L performed and designed experiments, analyzed data. I C-H performed experiments. AZ performed and designed experiments, analyzed data, wrote paper and conceived the project. The authors read and approved the final manuscript.

Acknowledgements

We thank the histology facility (Manolín and Marta) of the ISCIII for technical help.

References

1. King, TE Jr, Pardo A, Selman M. Idiopathic pulmonary fibrosis. Lancet. 2011 Dec 3; 378(9807): p. 1949-61.
2. Hecker L, Logsdon NJ, Kurundkar D, Kurundkar A, Bernard K, Hock T, Meldrum E, Sanders YY, Thannickal VJ. Reversal of persistent fibrosis in aging by targeting Nox4-Nrf2 redox imbalance. ci Transl Med. 2014 Apr 9; 6(231): p. 231ra47.
3. Lv XX, Wang XX, Li K, Wang ZY, Li Z, Lv Q, Fu XM, Hu ZW. Rupatadine protects against pulmonary fibrosis by attenuating PAF-mediated senescence in rodents. PLoS One. 2013 Jul 15; 8(7): p. e68631.
4. Shivshankar P, Brampton C, Miyasato S, Kasper M, Thannickal VJ, Le Saux CJ. Caveolin-1 deficiency protects from pulmonary fibrosis by modulating epithelial cell senescence in mice. Am J Respir Cell Mol Biol. 2012 Jul; 47(1): p. 28-36.
5. Ding N, Yu RT, Subramaniam N, Sherman MH, Wilson C, Rao R, Leblanc M, Coulter S, He M, Scott C, Lau SL, Atkins AR, Barish GD, Gunton JE, Liddle C, Downes M, Evans RM. A vitamin D receptor/SMAD genomic circuit gates hepatic fibrotic response. Cell. 2013 Apr 25; 153(3): p. 601-13.
6. Ito I, Waku T, Aoki M, Abe R, Nagai Y, Watanabe T, Nakajima Y, Ohkido I, Yokoyama K, Miyachi H, Shimizu T, Murayama A, Kishimoto H, Nagasawa K, Yanagisawa J. A nonclassical vitamin D receptor pathway suppresses renal fibrosis. J Clin Invest. 2013 Nov; 123(11): p. 4579-94.
7. Meredith A, Boroomand S, Carthy J, Luo Z, McManus B. 1,25 Dihydroxyvitamin D3 Inhibits TGFβ1-Mediated Primary Human Cardiac Myofibroblast Activation. PLoS One. 2015 Jun 10; 10(6): p. e0128655.
8. Zhang Z, Yu X, Fang X, Liang A, Yu Z, Gu P, Zeng Y, He J, Zhu H, Li S, Fan D, Han F, Zhang L, Yi X. Preventive effects of vitamin D treatment on bleomycin-induced pulmonary fibrosis. Sci Rep. 2015 Dec 2; 5: p. 17638.
9. Tan ZX, Chen YH, Xu S, Qin HY, Zhang C, Zhao H, Xu DX. Calcitriol inhibits bleomycin-induced early pulmonary inflammatory response and epithelial-mesenchymal transition in mice.. Toxicol Lett. 2016 Jan 5; 240(1): p. 161-71.
10. Guijarro T, Magro-Lopez E, Manso J, Garcia-Martinez R, Fernandez-Aceñero MJ, Liste I, Zambrano A. Detrimental pro-senescence effects of vitamin D on lung fibrosis.. Mol Med.. 2018 Dec 19; 24(1): p. 64.
11. Wyman C, Kanaar R. DNA double-strand break repair: all's well that ends well. Rev Genet.. 2006; 40: p. 363-83.
12. Campisi J, d'Adda di Fagagna F.. Cellular senescence: when bad things happen to good cells. Nat Rev Mol Cell Biol. 2007 Sep; 8(9): p. 729-40.
13. Aoshiba K, Tsuji T, Kameyama S, Itoh M, Semba S, Yamaguchi K, Nakamura H.. Senescence-associated secretory phenotype in a mouse model of bleomycin-induced lung injury.. Exp Toxicol

Pathol. 2013 Nov; 65(7-8): p. 1053-62..

14. Aoshiba K, Zhou F, Tsuji T, Nagai A.. DNA damage as a molecular link in the pathogenesis of COPD in smokers. Eur Respir J. 2012 Jun; 39(6): p. 1368-76.
15. Chilosi M, Carloni A, Rossi A, Poletti V.. Premature lung aging and cellular senescence in the pathogenesis of idiopathic pulmonary fibrosis and COPD/emphysema.. Transl Res. 2013; 162(3): p. 156–173.
16. Kuwano K, Araya J, Hara H, Minagawa S, Takasaka N, Ito S, Kobayashi K, Nakayama K. Cellular senescence and autophagy in the pathogenesis of chronic obstructive pulmonary disease (COPD) and idiopathic pulmonary fibrosis (IPF). Respir Investig.. 2016 Nov; 54(6): p. 397-406..
17. Leyssens C, Verlinden L, Verstuyf A. The future of vitamin D analogs. Front Physiol.. 2014 Apr 3; 5: p. 122.
18. Slatopolsky E, Finch J, Brown A.. New vitamin D analogs. Kidney Int Suppl. 2003 Jun; 85: p. S83-7..
19. Rogakou EP, Boon C, Redon C, Bonner WM.. Megabase chromatin domains involved in DNA double-strand breaks in vivo. J Cell Biol.. 1999 Sep 6; 146(5): p. 905-16.
20. Schultz LB, Chehab NH, Malikzay A, Halazonetis TD. p53 binding protein 1 (53BP1) is an early participant in the cellular response to DNA double-strand breaks. J Cell Biol.. 2000 Dec 25; 151(7): p. 1381-90..
21. Abraham RT. Checkpoint signalling: focusing on 53BP1. Nat Cell Biol.. 2002 Dec 4; 12: p. E277-9.
22. Zambrano A, García-Carpizo V, Gallardo ME, Villamuera R, Gómez-Ferrería MA, Pascual A, Buisine N, Sachs LM, Garesse R, Aranda A.. The thyroid hormone receptor β induces DNA damage and premature senescence.. J Cell Biol.. 2014 Jan 6; 204(1): p. 129-46.
23. Ward IM, Minn K, Jorda KG, Chen J.. Accumulation of checkpoint protein 53BP1 at DNA breaks involves its binding to phosphorylated histone H2AX.. J Biol Chem. 2003 May 30; 278(22): p. 19579-82.
24. Magro-Lopez E, Guijarro T, Martinez I, Martin-Vicente M, Liste I, Zambrano A. A Two-Dimensional Human Minilung System (Model) for Respiratory Syncytial Virus Infections.. Viruses. 2017 Dec 10; 9(12): p. 379.
25. Magro-Lopez E, Palmer C, Manso J, Liste I, Zambrano A.. Effects of lung and airway epithelial maturation cocktail on the structure of lung bud organoids.. Stem Cell Res Ther. 2018 Jul 11; 9(1): p. 186..
26. Huang SX, Green MD, de Carvalho AT, Mumau M, Chen YW, D'Souza SL, Snoeck HW.. The in vitro generation of lung and airway progenitor cells from human pluripotent stem cells. Nat Protoc. 2015 Mar; 10(3): p. 413-25.
27. Huang SX, Islam MN, O'Neill J, Hu Z, Yang YG, Chen YW, Mumau M, Green MD, Vunjak-Novakovic G, Bhattacharya J, Snoeck HW.. Efficient generation of lung and airway epithelial cells from human pluripotent stem cells.. Nat Biotechnol. 2014 Jan; 32(1): p. 84-91..

28. Chen YW, Huang SX, de Carvalho ALRT, Ho SH, Islam MN, Volpi S, Notarangelo LD, Ciancanelli M, Casanova JL, Bhattacharya J, Liang AF, Palermo LM, Porotto M, Moscona A, Snoeck HW.. A three-dimensional model of human lung development and disease from pluripotent stem cells.. Nat Cell Biol. 2017 May; 19(5): p. 542-549..
29. Martínez I, García-Carpizo V, Guijarro T, García-Gomez A, Navarro D, Aranda A, Zambrano A.. nduction of DNA double-strand breaks and cellular senescence by human respiratory syncytial virus.. Virulence. 2016 May 18; 7(4): p. 427-42..

Figures

Figure 1 Magro-Lopez et al.

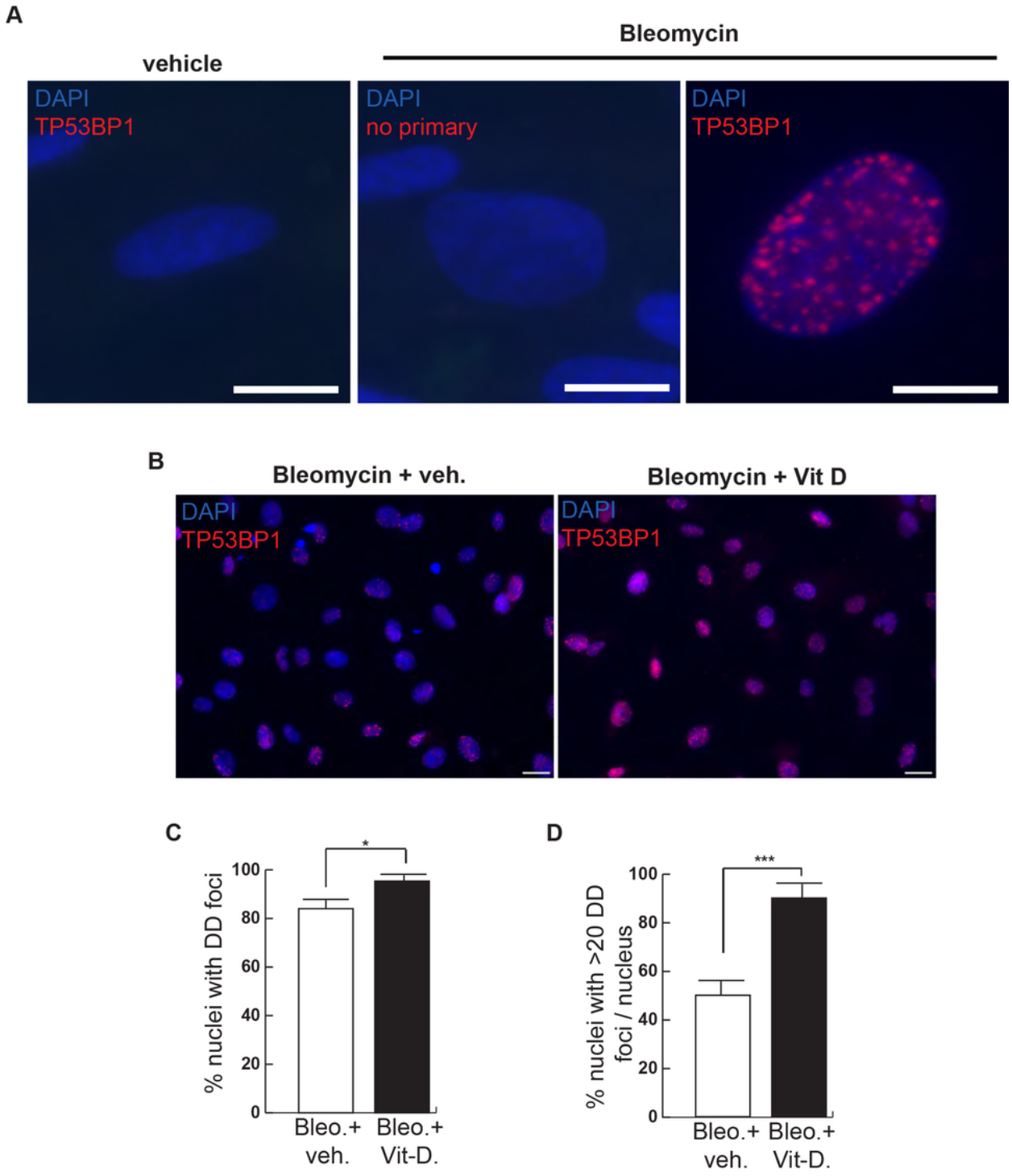

Figure 1

Effects of bleomycin and vitamin D in A549 cells. A. A549 cells were treated with 25 µg/mL of bleomycin for 48h and then processed for indirect immunofluorescence to detect DNA damage foci containing TP53BP1 (red dots), a reliable marker of DNA double-strand breaks (DSBs). veh: Bleomycin vehicle (PBS). No primary: negative control of the immunofluorescence assay consisting of the absence of primary antibody. Scale bar: 5 µm. B. Expression of DSBs [TP53BP1 foci (red dots)] induced by vitamin D in the

presence of bleomycin. A549 cells were pretreated with 5 nmol/L vitamin D for 2 h, subjected to a bleomycin shock (12 µg/mL for 6 h) and then treated with 5 nmol/L vitamin D or its vehicle. Representative micrographs taken at 48 h post-shock are shown. Scale bar: 20 µm. C-D. Quantification of damaged cell: % of nuclei with TP53BP1 foci (C) or % of severely damaged cells [more than 20 TP53BP1 foci per nucleus (D)]. Data from three experiments are represented; more than 150 cells per condition were analyzed (P<0,001).

Figure 2 Magro-Lopez et al.

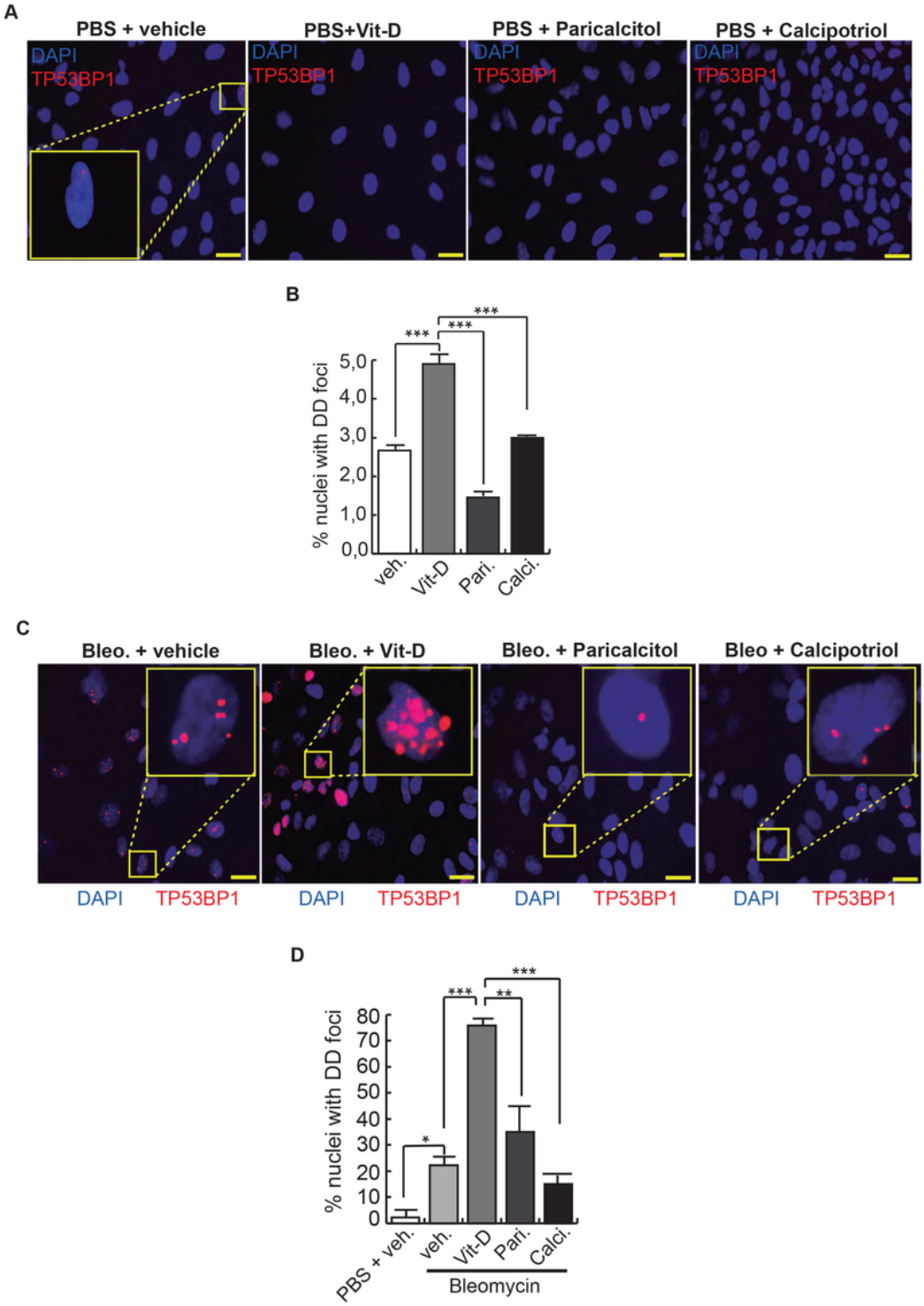

Figure 2

Effects of vitamin D and two hypocalcemic analogs in the expression of DNA damage induced by bleomycin in A549 cells. A. Basal expression of DSBs (TP53BP1 foci (red dots)) induced by vitamin D and the analogs paricalcitol and calcipotriol in the absence of bleomycin. A549 cells were treated with 50 nmol/L vitamin D (or the corresponding analog) for 48 h and then subjected to immunofluorescence to detect DD foci. Representative micrographs are shown. PBS is the bleomycin vehicle; vehicle: vitamin D or analogs vehicle; scale bar: 100μm. B. Quantification of damaged cells (nuclei with TP53BP1 foci). Data from three experiments are represented; more than 150 cells per condition were analyzed. ANOVA P<0,001. C. Expression of TP53BP1 foci (red dots) in cultures of A549 cells pretreated with 50 nmol/L vitamin D, analogs or its vehicle for 2h and subjected to a bleomycin shock (12 μg/mL) for 6h. After that, the cultures were treated with 50 nmol/L vitamin D and the analogs paricalcitol and calcipotriol (or vehicle) for 48h. Representative micrographs taken at 48h post-shock are shown. Scale bar: 100μm. D. Quantification of damaged cells; veh: vitamin D or analogs vehicle. Data from three experiments are represented; more than 150 cells per condition were analyzed; ANOVA P<0,001. The results presented in the figures are means ± SEM. Significance of the analysis is indicated as, *: P<0.05, **: P<0.01, ***: p<0.001.

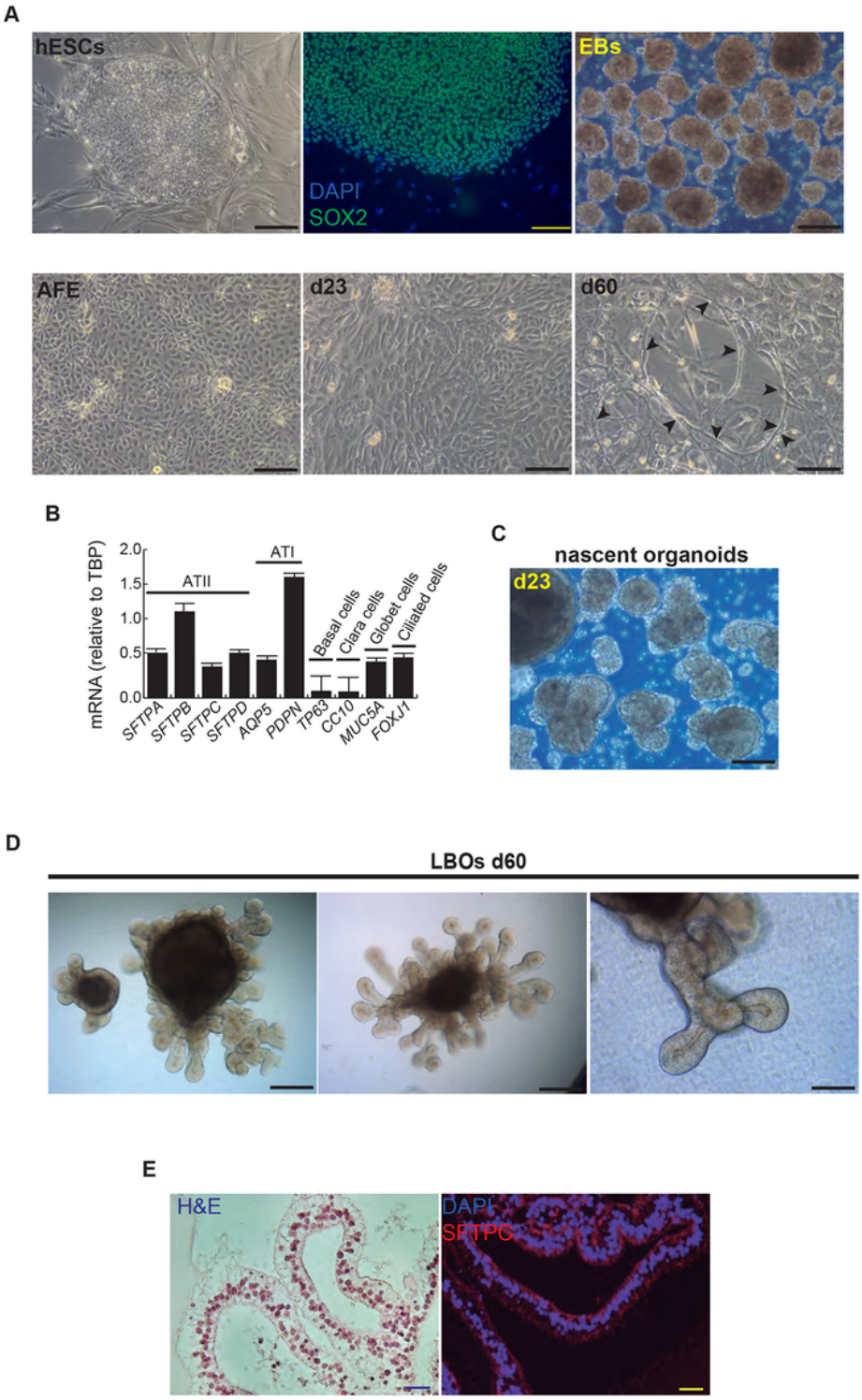

Figure 3

Representative micrographs of the sequential differentiation processes and expression markers. (A) left upper micrograph: AND-2 colony growing along with feeder cells [inactivated MEFs (iMEFs)]; scale bar: 100 μm); central upper micrograph: expression of SOX2 (SRY (Sex Determining Region Y)-box 2) in an undifferentiated colony of AND-2; scale bar: 100 μm). Right upper micrograph: Representative micrograph of EBs (embryoid bodies). Bottom panels: AFE (anterior foregut endoderm) and representative

micrographs of cultures at day 23 of differentiation (lung progenitors) and at day 60 (differentiated lung and airway cells): Black arrowheads signal cells with a typical flat and crescent shape morphology denoting alveolar type I cells (ATI cells); scale bar: 100 µm. B. Levels of expression [relative to TBP (TATA Box Binding Protein)] of lung and airway epithelial cells markers at day 60 (n=3; > 4 organoids per condition were used). C. Representative micrograph of nascent organoids growing in suspension at day 23. D. Representative micrograph of LBOs at day 50 embedded in MatrigelTM sandwiches; scale bar: 100 µm and 50 µm (micrograph on the right). E. Micrograph on the left: Histochemical analysis of LBO sections (H&E staining); representative micrograph of an immunohistochemical staining of LBO sections (micrographon the right) with a SFTP-C antibody. Scale bar: 100 µm.

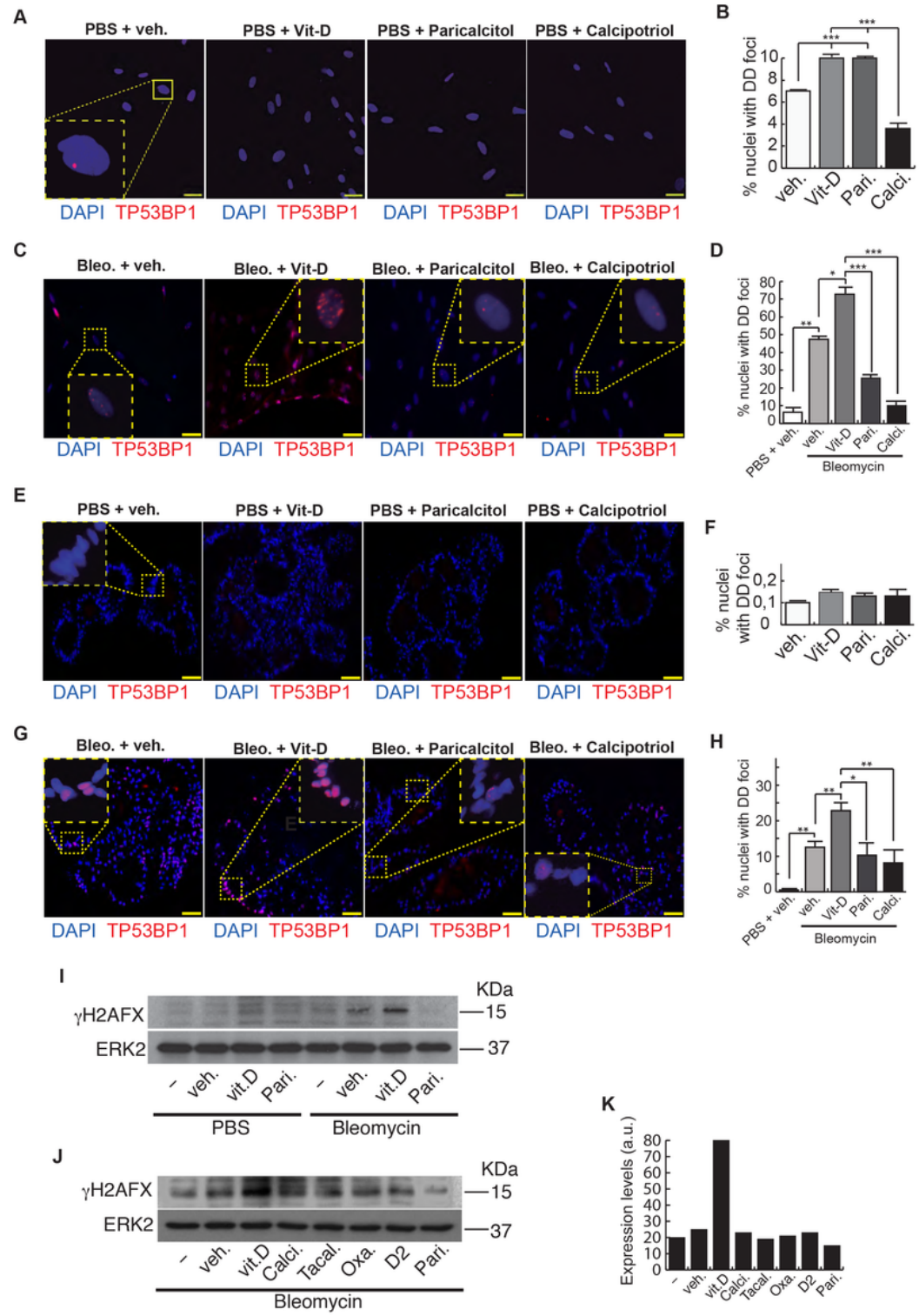

Figure 4

Effects of vitamin D and hypocalcemic analogs in the expression of DNA damage induced by bleomycin in the minilungs generated from hESCs. A. Basal expression of DNA damage (TP53BP1 foci (red dots)) induced by vitamin D and the analogs paricalcitol and calcipotriol in the absence of bleomycin. 2D minilungs were treated with 50 nmol/L vitamin D (or the corresponding analog) for 72 h and then subjected to immunofluorescence to detect DD foci. Representative micrographs are shown. PBS is the

bleomycin vehicle; veh.: vitamin D or analogs vehicle; scale bar: 100μm. B. Quantification of damaged cells (nuclei harboring TP53BP1 foci) corresponding to conditions A; (n=3; >150 cells were analyzed; ANOVA P<0,001). C. Expression of TP53BP1 foci (red dots) in 2D minilungs cells pretreated with 50 nmol/L vitamin D, analogs or its vehicle for 2h and then with bleomycin (12,5 μg/mL), vitamin D or analogs (50 nmol/L) for 72h. After that, the cultures were processed for indirect immunofluorescence to detect DNA damage foci containing TP53BP1 (red dots); representative micrographs are shown. Scale bar: 100μm. D. Quantification of damaged cells corresponding to conditions C. veh: vitamin D or analogs vehicle; (n=3; >150 cells were analyzed; ANOVA P<0,001). E. Basal expression of DNA damage in 3D minilungs (LBOs): TP53BP1 foci (red dots) induced by vitamin D and the analogs paricalcitol and calcipotriol in the absence of bleomycin. 3D minilungs (LBOs) were treated with 50 nmol/L vitamin D (or the corresponding analog) for 72 h and then subjected to immunofluorescence to detect DD foci. Representative micrographs are shown. PBS is the bleomycin vehicle; veh.: vitamin D or analogs vehicle; scale bar: 100μm. F. Quantification of damaged cells corresponding to condition E (nuclei harboring TP53BP1 foci); (n=3; >4 organoids per condition were used and >150 cells were analyzed; ANOVA P>0,05). G. Expression of TP53BP1 foci (red dots) in 3D minilungs (LBOs) cells pretreated with 50 nmol/L vitamin D, analogs or its vehicle for 2h and then with bleomycin (25 μg/mL), vitamin D or analogs (50 nmol/L) for 72h. After that, the cultures were processed for indirect immunofluorescence to detect DNA damage foci containing TP53BP1 (red dots); representative micrographs are shown. Scale bar: 100μm. H. Quantification of damaged cells corresponding to condition G (nuclei harboring TP53BP1 foci); (n=3; >4 organoids per condition were used and >150 cells were analyzed; ANOVA P<0,001). The results presented in the figures are means ± SEM. Significance of the analysis is indicated as, *: P<0.05, **: P<0.01, ***: p<0.001. I. Detection of γH2AFX in A549 cell extracts. Cells were pretreated with 50 nmol/L vitamin D for 2 h, subjected to a bleomycin shock (12 μg/mL for 6 h) and then treated with 50 nmol/L vitamin D or its vehicle. Cell extracts were obtained at 48 h post-shock; Pari: paricalcitol; ERK2 was used as loading control. KDa: kilodaltons. J. Detection of γH2AFX in A549 cell extracts. Cells were treated as in J. Cell extracts were obtained at 48 h post-shock; Calci: calcipotriol; Tacal: tacalcitol; Oxa.: 22-oxacalcitriol; D2: vitamin D2; Pari: paricalcitol; ERK2 was used as loading control. KDa: kilodaltons. K: densitometry analysis of western J; a.u: arbitrary units.